

Code Division Multiple-Access Techniques in Optical Fiber Networks—Part II: Systems Performance Analysis

JAWAD A. SALEHI, MEMBER, IEEE, AND CHARLES A. BRACKETT, MEMBER, IEEE

Abstract—In Part I of this paper, we investigated a technique to establish fiber-optic-code division multiple-access (FO-CDMA) communications system. In particular, we discussed the need for a new class of signature sequences that satisfy the auto- and crosscorrelation properties that are essential for a successful FO-CDMA system. We introduced a new class of sequences that are called optical orthogonal codes (OOC's). Furthermore, we investigated the probability density function for any two interfering OOC's. In Part II of this paper, we utilize the results of Part I to derive the bit error rate of the proposed FO-CDMA system as a function of data rate, code length, code weight, number of users, and receiver threshold; and we discuss the performance characteristics for a variety of system parameters. Furthermore, we discuss a means of reducing the effective multiple-access interference signal by placing an optical hard-limiter at the front end of the desired optical correlator. We calculate the performance of the FO-CDMA with an ideal optical hard-limiter, and we show that using an optical hard-limiter would, in general, improve system performance.

I. INTRODUCTION

IN [1], we investigated fiber-optic code division multiple-access communications systems. Our goal was to take the full advantage of fiber-optic signal processing techniques to establish an all optical code division multiple-access communications systems. In particular, we discussed the need for a new class of sequences (signature sequences) that satisfy the auto- and crosscorrelation properties for a typical FO-CDMA system. We introduced such sequences, namely, optical orthogonal codes (OOC's) [1], [2], that satisfy the above two properties. We reported an experiment in which we demonstrated the auto- and crosscorrelation properties of these newly invented codes, and their use in a FO-CDMA system. Furthermore, we derived the probability distribution function of any two interfering OOC's as a function of their code length, weight, and the relative positions of their respective pulses. We presented a detailed study of different interference patterns from which the strongest and the weakest interference patterns were introduced.

In this paper, we study a mathematical development of the probability of error per bit for FO-CDMA using OOC's. In Section II, we define and analyze the interference signals, which are an inherent part of these kinds of networks. In Section III, we evaluate the probability density functions associated with the sum of these undesired signals (interference signals). In Section IV, we calculate the bit error rate for FO-CDMA as a function of key parameters, namely bandwidth expansion factor F (processing gain); number of pulses K in code; the number of users N ; and Th , the threshold. In

Section V, we discuss a means of reducing the effect of the undesired signals, i.e., the use of an ideal optical hard-limiter (optical nonlinear threshold element). We show, for example, that under certain conditions, using an ideal optical hard-limiter in FO-CDMA would improve the system's performance by some orders of magnitude. Finally, in Appendix A we discuss the equivalence of two interfering OOC's and their corresponding optical disk patterns [1].

ON-OFF FIBER-OPTIC CODE DIVISION MULTIPLE ACCESS

In a typical FO-CDMA communications network there would be N transmitter and receiver pairs (users). Fig. 1 shows one such network in a star configuration. For the performance analysis, i.e., the bit error rate, we consider the simplest network protocol; it is assumed that the communication between the transmitters and receivers is pairwise, and communications between each n th, for $1 \leq n \leq N$, transmitter and receiver pair is continuous. In our system performance evaluation, the performance degradation is due only to the effects of the presence of other users. The effects of quantum noise and thermal noise are neglected. All light sources are incoherent. As a result, the optical light intensity of multiple users occurring at the same time would add in intensity. Furthermore, all users have the same effective average power at any receiver so that one user could not overwhelm the others, and all users have identical bit rate and signal format.

The n th baseband signal $s_n(t)$ at the output of the n th optical encoder, is given by

$$s_n(t) = s_n b_n(t) DP_n(t) \quad (1)$$

where s_n , $b_n(t)$, and $DP_n(t)$ are the n th user's transmitted optical intensity, binary data signal, and OOC, respectively.

The n th user's binary data signal $b_n(t)$ for continuous communication is given by

$$b_n(t) = \sum_{l=-\infty}^{\infty} b_l^{(n)} P_T(t-lT) \quad (2)$$

where $b^{(n)} = (b_l^{(n)})$ is the n th data sequence that takes on 0 or 1 (on-off keying) for each l with equal probability and $P_T(t)$ is the rectangular pulse of duration T which starts at $t = 0$. Furthermore, $DP_n(t)$, the n th user's OOC (signature sequence), is given by

$$DP_n(t) = \sum_{j=-\infty}^{\infty} A_j^{(n)} P_{T_c}(t-jT_c) \quad (3)$$

where $P_{T_c}(t)$ is the rectangular pulse of duration T_c and $A^{(n)} = (A_j^{(n)})$ is the n th periodic sequence of binary optical pulses (0, +1) with period (length) $F = T/T_c$, i.e., $A_{j+F}^{(n)} = A_j^{(n)}$, and weight K [1]. The transmitters are not time synchronous (with each other), thus, as illustrated by Fig. 1, the received

Paper approved by the Editor for CATV of the IEEE Communications Society. Manuscript received January 15, 1988; revised March 24, 1989. This paper was presented in part at ICC'87, MILCOM '87, and the Information Theory Symposium '88.

The authors are with Bell Communications Research, Morristown, NJ 07961-1910.

IEEE Log Number 8929099.

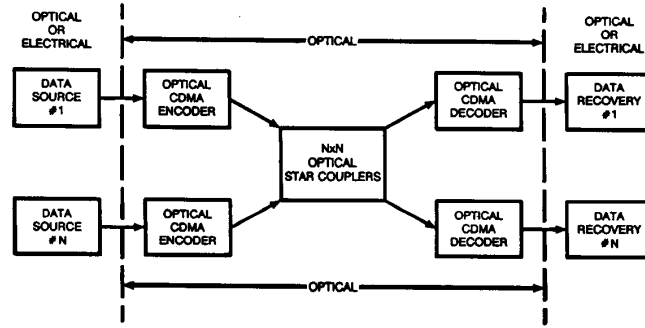


Fig. 1. A typical fiber-optic code division multiple-access (FO-CDMA) network in a star configuration.

signal at the front end of each receiver is of the form

$$r(t) = \sum_{n=1}^N s_n(t - \tau_n) \quad (4)$$

where τ_n is the time-delay associated with the n th signal. From (1) and (4) we have

$$r(t) = \sum_{n=1}^N b_n(t - \tau_n) DP_n(t - \tau_n). \quad (5)$$

We have assumed $s_n = 1$ in (1) for $1 \leq n \leq N$ (equal amplitudes assumption). We assume $\tau_n = 0$ in the analysis of the receiver that is matched to the n th signal. In addition, $0 \leq |\tau_n| \leq T$, for $1 \leq n \leq N$. The n th receiver is assumed to be a correlation receiver (or matched filter) that is matched to the n th signal [3]. In fiber-optic signal processing, the n th correlation process can be established by an all passive fiber optic tapped delay line [4], with an impulse response equivalent to the time reversal of the n th OOC, followed by an ideal photodetector and a sampler. For notational simplicity, we assume that the desired user's signal is denoted by $n = 1$ in (5). Fig. 2(a) shows a typical optical correlator for user 1 and Fig. 2(b) shows its equivalent optical matched filter where Z_1 is the sampled output of both the optical correlator and its equivalent matched filter at time $t = T$. The effect of the n th user's signal on the first receiver is denoted by $I_n^{(1)}$. Hence, Z_1 , the output of the first user's correlator at time T , can be written as

$$Z_1 = \frac{1}{T_c} \int_0^T r(t) DP_1(t) dt = b_0^{(1)} K + I_1 \quad (6)$$

where $b_0^{(1)}$ is the zeroth data of the first user that can take on two values, namely, 0 or 1 with equal probability. The first term of (6), $b_0^{(1)} K$, is desired signal term and the second term, $I_1 = \sum_{n=2}^N I_n^{(1)}$, is the undesired signal term (total interference signal) at the output of the desired receiver's correlator, i.e., the first receiver. Note that, the undesired signal I_1 is composed of $(N - 1)$ interference signals $I_n^{(1)}$ where each $I_n^{(1)}$ is random variable (see Appendix A) with mean $M_{I_n^{(1)}}$ and variance $\sigma_{I_n^{(1)}}^2$. If the $I_n^{(1)}$ are independent and identically distributed random variables, then the mean M_{I_1} and the variance $\sigma_{I_1}^2$ of the total interference signal I_1 can be expressed as

$$M_{I_1} = (N - 1)M \quad (7)$$

and

$$\sigma_{I_1}^2 = (N - 1)\sigma^2 \quad (8)$$

where $M = M_{I_n^{(1)}}$ and $\sigma^2 = \sigma_{I_n^{(1)}}^2$ for $2 \leq n \leq N$.

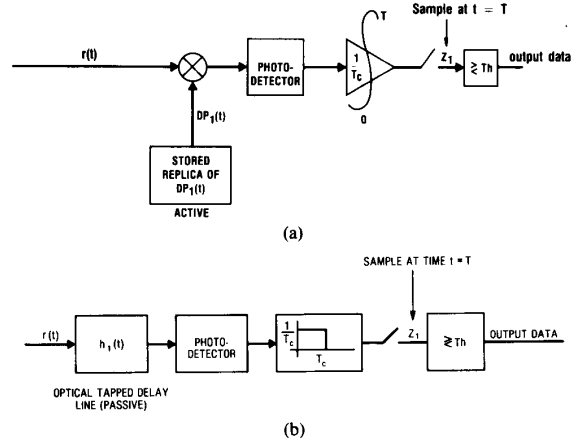


Fig. 2. (a) An ideal optical correlator using active optical components. (b) The equivalent optical matched filter.

III. PROBABILITY DENSITY FUNCTION FOR INTERFERENCE SIGNAL I_1

In evaluating the probability density function for the interference signal I_1 we will consider two cases: A) chip synchronous and B) ideal chip asynchronous that assumes that there are no adjacent pulses among any two OOC's (see [1, Section V]). As it was discussed in [1], the above considerations stem from the fact that the evaluation of the exact probability density function for I_1 could required the knowledge of probability density functions associated with each $I_n^{(1)}$'s for $2 \leq n \leq N$. And since there are N users in a FO-CDMA system and the interference I_j at the output of the j th receiver contains $(N - 1)$ interference terms then a total knowledge of $N(N - 1)/2$ probability density functions would be required. The task of evaluating $N(N - 1)/2$ probability density functions is lengthy and tedious especially for large N . Therefore, we have chosen the above two extreme cases, i.e., Case A) (chip synchronous interference), and Case B) (ideal chip asynchronous interference), for the analysis of interfering signals in order to make the following calculations on their probability density functions and the associated probability of error per bit (PE) mathematically more general and convenient. Note that because of the relationship on the variances, the PE derived from Case A) would be an upper bound on the exact PE and the PE derived from Case B) would be a lower bound on the exact PE, i.e.,

$$PE [\text{Case B}] \leq PE (\text{exact}) < PE [\text{Case A}] \quad (9)$$

The interference signal I_1 is the sum of $N - 1$ independent identically distributed random variables, $I_n^{(1)}$. Therefore, the

probability density function for I_1 , $P_{I_1}(I_1)$, is the convolution of the probability density functions of random variables $I_n^{(1)}$ for $2 \leq n \leq N$. The probability density functions for interference signal I_1 for the above two cases are expressed as follows.

Case A) Chip Synchronous:

$$P_{I_1}(I_1) = \sum_{i=0}^{N-1} \binom{N-1}{i} \left(\frac{K^2}{2F}\right)^i \cdot \left(1 - \frac{K^2}{2F}\right)^{N-1-i} \delta(I_1 - i). \quad (10)$$

Case B) Ideal Chip Asynchronous:

$$P_{I_1}(I_1) = q^{N-1} \delta(I_1) + (N-1)pq^{N-2} |I_1| + \binom{N-1}{2} p^2 q^{N-3} f(I_1) + \sum_{i=3}^{N-1} \binom{N-1}{i} p^i q^{N-1-i} G\left(\frac{i}{2}, \frac{i}{12}\right) \quad (11)$$

where $p \triangleq K^2/F$, $q \triangleq 1 - K^2/F$ and

$$|I_1| \triangleq \begin{cases} 1 & 0 < I_1 < 1 \\ 0 & \text{elsewhere} \end{cases} \quad (12)$$

and

$$f(I_1) \triangleq \begin{cases} 1 - |I_1 - 1| & 0 \leq I_1 \leq 2 \\ 0 & \text{elsewhere} \end{cases} \quad (13)$$

and $G(i/2, i/12)$ is a Gaussian density function with mean $i/2$ and variance $i/12$.

IV. PROBABILITY OF ERROR

The exact probability of error per bit, PE (exact), is defined as

$$PE \text{ (exact)} = \Pr(Z_1 \geq Th/b_0^{(1)} = 0) \cdot \Pr(b_0^{(1)} = 0) + \Pr(Z_1 < Th/b_0^{(1)} = 1) \cdot \Pr(b_0^{(1)} = 1) \quad (14)$$

where Th is defined as the threshold. The second term of (14) is zero for $0 \leq Th \leq K$ because $\Pr(Z_1 < Th/b_0^{(1)} = 1) = \Pr(K - Th + I_1 < 0) = \Pr(\eta < 0)$ where $\eta = K - Th + I_1$ is a nonnegative definite random variable that cannot take on any negative value. Therefore, the probability of error when $b_0^{(1)} = 1$ is zero. But when $b_0^{(1)} = 0$, the above argument is not true and errors could occur. These errors are the first term of (14), i.e.,

$$PE \text{ (exact)} = \frac{1}{2} \int_{Th}^{\infty} P_{I_1}(I_1) dI_1. \quad (15)$$

Case A) Chip Synchronous (An Upper Bound): In this case the probability of error is expressed as

$$PE \text{ [Case A]} = \frac{1}{2} \sum_{i=Th}^{N-1} \binom{N-1}{i} \cdot \left(\frac{K^2}{2F}\right)^i \left(1 - \frac{K^2}{2F}\right)^{N-1-i}. \quad (16)$$

Fig. 3(a) shows the PE [Case A] versus the threshold for a fixed number of users ($N = 20$) and weight ($K = 5$) and different values of chip size. As expected, when the number of chips per frame, F , decreases, the system performance degrades, or vice versa. But the margin (rate) of degradation

or improvement is low. A more interesting result is depicted in Fig. 3(b) where PE [Case A] versus the threshold is shown for a fixed number of users $N(10)$ and chip size $F(1000)$, but, for different values of $K(K = 1, 3, 5, 7, 9)$. For $K = 1$, the threshold is set at 1, and one achieves an error rate of $\approx 2.1 \times 10^{-3}$. If it is desired to improve the system performance, it would be required to use more pulses in the sequences. With more pulses, it is possible to push up the threshold level. If the number of pulses is increased and the threshold level is kept low as for the previous case, the system performance degrades since, by increasing the number of pulses in a frame, one introduces a more dense channel and increases the probability of hitting an intended chip (K^2/F). But as the threshold level gets higher, the system performance improves since it becomes less probable that multiple users will occupy a particular chip to the level of the threshold. This characteristic of the performance of FO-CDMA using OOC's is observed in Fig. 3(b). For example, when the K goes to 9 and when the threshold is kept at 1, the system performance with respect to $K = 1$ is degraded, but as the threshold level gets bigger, the system performance improves. For $K = 9$, $Th = 9$ the error reaches to $\approx 10^{-13}$. This error rate is about ten orders of magnitude better than when $K = 1$.

A special case arises when the number of pulses in the OOC's gets larger than the number of users. In this case, one can ideally maintain the error due to the interference to be zero. For example, if $F = 1000$, $N = 10$, $K = 10$, and $Th = 10$ then, ideally, the error due to the interference signal is zero because the maximum value that the interference signal can have is $N - 1 = 9$, which is always less than $Th = 10$.

Fig. 3(c) shows PE [Case A] versus the threshold for a fixed number of chips, $F = 1000$, and weights, $K = 5$, and for a different number of users, i.e., N . At $Th = 5$ and $N = 10$, PE [Case A] = 1.8×10^{-8} , and for the same threshold value when $N = 50$, PE [Case A] = 1.8×10^{-4} . This is equivalent to four orders of magnitude in performance degradation.

Case B) Ideal Chip Asynchronous (A Lower Bound):

$$PE \text{ [Case B]} = \frac{1}{2} \left[q^{N-1} \int_{Th}^{\infty} \delta(I_1) dI_1 + (N-1)pq^{N-2} \cdot \int_{Th}^{\infty} |I_1| dI_1 + \binom{N-1}{2} p^2 q^{N-3} \cdot \int_{Th}^{\infty} f(I_1) dI_1 + \sum_{i=3}^{N-1} \binom{N-1}{i} \cdot p^i q^{N-1-i} Q\left(\frac{Th - \frac{i}{2}}{\sqrt{\frac{i}{12}}}\right) \right] \quad (17)$$

where $Q(x)$ is the Gaussian integral function and it is defined as

$$Q(x) \triangleq \frac{1}{\sqrt{2\pi}} \int_x^{\infty} \exp\left(-\frac{\mu^2}{2}\right) d\mu. \quad (18)$$

Fig. 4 shows PE [Case B] of (17) versus the threshold for fixed values of $N(10)$ and $F(1000)$ and for different values of $K(1, 3, 5, 7, 9)$. As expected, the system performance of chip asynchronous FO-CDMA, PE [Case B], is superior to its chip synchronous case, PE [Case A]. For example, for $K =$

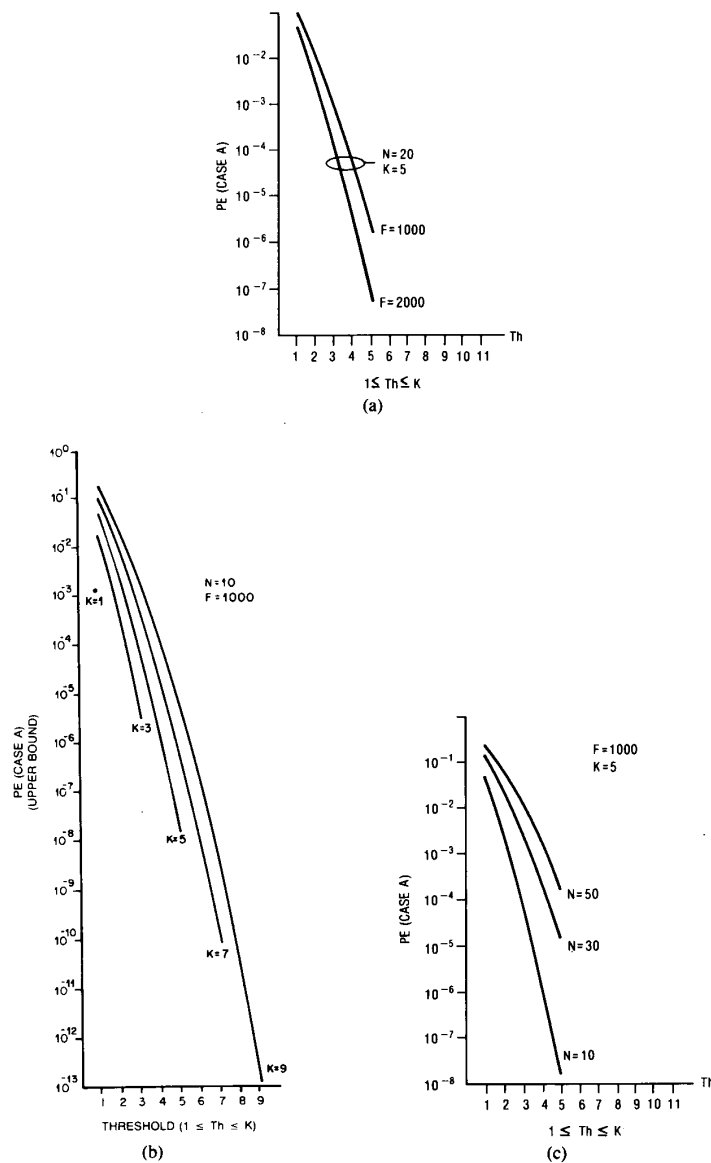


Fig. 3. (a) Upper bound on bit error rate performance versus threshold for $N = 20$, $K = 5$, and $F = 1000, 2000$. (b) Upper bound on bit error rate performance versus threshold for $N = 10$, $F = 1000$ and for different values of $K = 1, 3, 5, 7, 9$. (c) Upper bound on bit error rate performance versus threshold for $F = 1000$, $K = 5$ and $N = 50, 30, 10$.

5 and $Th = 5$ PE [Case A] is $\approx 1.8 \times 10^{-8}$ [Fig. 3(b)] whereas for the same sets of design parameters K and Th , system bit error rate for ideal chip asynchronous, PE [Case B)], case reduces to $\approx 5.7 \times 10^{-11}$. This is two to three orders of magnitude improvement in the system performance. Intuitively, one can argue that in the ideal chip asynchronous case it takes at least two users' signals to occupy one chip pulse of the desired user's signal where in the synchronous case, a chip of the desired user can be occupied by only one interference signal. Therefore, the effective number of interference signals in the ideal asynchronous case is less than the synchronous case. This reduction in effective number of interference signals contributes to better error rates for the asynchronous case. As in the synchronous case, PE [Case B)] behaves in a

similar fashion, that is, the system performance improves when the number of pulses in the sequences, i.e., OOC, is increased and at the same time the threshold level is increased.

V. OPTICAL HARD-LIMITER

One way to improve the system performance of FO-CDMA is by reducing the effect of the interference signal intensity. One way to reduce this interference effect is by placing an optical hard-limiter (optical threshold element [5]) before the optical tapped-delay line. An ideal optical hard-limiter is defined as

$$g(x) = \begin{cases} 1, & x \geq 1 \\ 0, & 0 \leq x < 1 \end{cases} \quad (19)$$

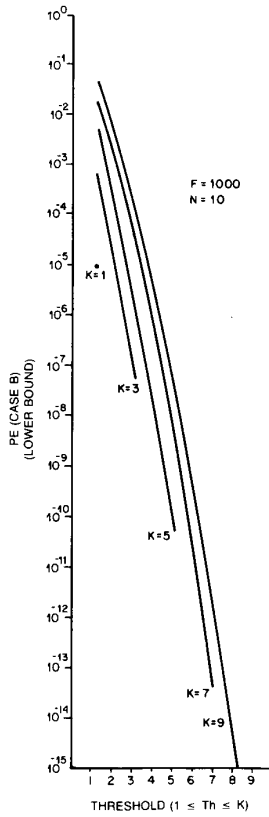


Fig. 4. Lower bound on bit error rate performance versus threshold for $N = 10$, $F = 1000$, and $K = 1, 3, 5, 7, 9$.

Therefore, if an optical light intensity (x) is bigger than or equal to one,¹ the hard-limiter would clip the intensity back to one, and if the optical light intensity is smaller than one, the response of the optical hard-limiter would be zero. This ideal nonlinear process would enhance the system performance because it would exclude some combinations of interference patterns from causing errors as in the soft-limiter case, i.e., the patterns that caused errors by analog summation of light intensity rather than by exact reproduction of the particular pattern with no analog effect. For example, an OOC $A' = [1011000100000]$ has a maximum value of "4" at the output of its matched filter (correlator). An interference pattern (sequence) of the form $[3000000100000]$ would have maximum value of "4" at the output of the A' correlator, which could cause an error if the threshold is set at 4. But if the interference pattern is hard-limited, then it would reduce to $[1000000100000]$. This pattern has a maximum value of 2 at the correlation time and it would not cause an error at the output of decision circuit when the threshold is at 4.

In general, the received signal $r(t)$ of (4) is passed through an optical hard-limiter (see Fig. 5) before it is correlated with the desired receiver's optical correlator. Hence, the interference I_1 at the output of the desired correlator (first user) can be expressed as

$$I_1 = \frac{1}{T_c} \int_0^T g(I_1(t)) DP_1(t) dt$$

$$= \sum_{j=0}^{F-1} V_j^{(1)} A_j^{(1)} \quad (20)$$

¹ In this case "one" is a normalized value for a given fixed intensity.

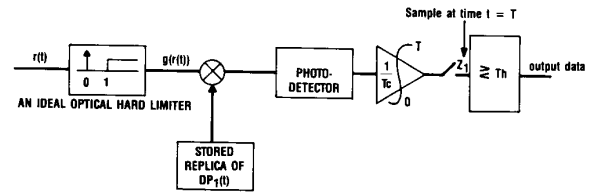


Fig. 5. A typical optical receiver with an ideal optical hard-limiter.

where

$$I_1(t) \triangleq \sum_{n=2}^N s_n(t - \tau_n) \quad (21)$$

and $V_j^{(1)}$ is defined as

$$V_j^{(1)} = \frac{1}{T_c} \int_{jT_c}^{(j+1)T_c} g(I_1(t)) dt. \quad (22)$$

A. Probability Density Function for the Random Variable $V_j^{(1)}$

Case A) Chip Synchronous: $V_j^{(1)}$, for chip synchronous is expressed as

$$V_j^{(1)} \triangleq \begin{cases} 1 & \text{if } I_1(t) \geq 1 \text{ for } jT_c \leq t \leq (j+1)T_c \\ 0 & \text{if } I_1(t) = 0 \text{ for } jT_c \leq t \leq (j+1)T_c \end{cases} \quad (23)$$

Therefore, the probability density function for the random variable $V_j^{(1)}$ is

$$P_{V_j^{(1)}}(V_j^{(1)}) = q' \delta(V_j^{(1)}) + p' \delta(V_j^{(1)} - 1) \quad (24)$$

where, from (10)

$$q' \triangleq \Pr [I_1(t) = 0 \text{ for } jT_c \leq t \leq (j+1)T_c] = q^{N-1} \quad (25)$$

and similarly

$$p' \triangleq \Pr (I_1(t) \geq 1 \text{ for } jT_c \leq t \leq (j+1)T_c) \\ = 1 - \Pr (I_1(t) = 0 \text{ for } jT_c \leq t \leq (j+1)T_c) \\ = 1 - q' \quad (26)$$

where q and p for hard-limiting case are defined as

$$q \triangleq \Pr (b_o^{(n)} A_j^{(n)} = 0) = 1 - \frac{K}{2F} \quad (27)$$

and

$$p \triangleq \Pr (b_o^{(n)} A_j^{(n)} = 1) = \frac{K}{2F} = 1 - q \quad (28)$$

where $b_o^{(n)}$ corresponds to the zeroth data of the n th user that can take on two values 1 or 0 each with probability 1/2. And $A_j^{(n)}$ corresponds to the j th position of the n th user's OOC and it also takes on two values 1 or 0 with $\Pr (A_j^{(n)} = 1) = K/F$ and $\Pr (A_j^{(n)} = 0) = 1 - K/F$.

Case B) Ideal Chip Asynchronous: For ideal chip asynchronous [1], $V_j^{(1)}$ is defined as

$$V_j^{(1)} = \begin{cases} 0 < V_j^{(1)} \leq 1 & \text{if } I_1(t) > 0 \text{ for } jT_c \leq t \leq (j+1)T_c \\ 0 & \text{if } I_1(t) = 0 \text{ for } jT_c \leq t \leq (j+1)T_c \end{cases} \quad (29)$$

Therefore, the probability density function for the above random variable $V_j^{(1)}$ is

$$P_{V_j^{(1)}}(V_j^{(1)}) = q' \delta(V_j^{(1)}) + p' |\overline{V_j^{(1)}}| \quad (30)$$

where

$$\begin{aligned} q' &\triangleq \Pr(I_1(t)=0 \text{ within a chip time}) \\ &= q^{N-1} \end{aligned} \quad (31)$$

and

$$\begin{aligned} p' &\triangleq \Pr(I_1(t)>0 \text{ within a chip time}) \\ &= 1 - q^{N-1} \end{aligned} \quad (32)$$

where q and p for chip asynchronous are defined as

$$q \triangleq 1 - \frac{K}{F} = 1 - p. \quad (33)$$

B. Upper and Lower Bounds on PE for FO-CDMA with Optical Hard-Limiter

In this section, we will derive upper and lower bounds on PE instead of calculating the exact expressions for it. Derivations for the exact expressions for PE [Case A] with an optical hard-limiter] and PE [Case B] with an optical hard-limiter] are mathematically complicated due to the highly correlated events $V_j^{(n)}$ for all $1 \leq n \leq N-1$ and $0 \leq j \leq F-1$. But a less complicated expression can be obtained as upperbounds to both cases.

Case A) Chip Synchronous: In this case, an error occurs when the desired transmitter sends a zero and the interference signal, due to the other users, reproduces the desired pattern up to the threshold or higher at the front end of the desired fiber optic tapped-delay line. There are $\binom{K}{Th}$ ways of reproducing a pattern with K pulses up to the threshold level Th . An upperbound can be achieved by assuming that a particular chip position of a desired sequence is hit for the first time with probability $p' = 1 - q^{N-1}$. Then the next chip position of the desired pattern will be hit with one less effective number of the total interference signal, i.e., $1 - q^{N-2}$ is the probability that one of the remaining $K-1$ chips would be hit, etc. Therefore, an upperbound can be expressed as

PE [Case A] with optical hard-limiter]

$$\leq \frac{1}{2} \left(\frac{K}{Th} \right) \prod_{m=0}^{Th-1} (1 - q^{N-1-m}) \quad (34)$$

where the symbol Π denotes the product, and q is defined as in (27). Fig. 6(a)–(c) show the FO-CDMA system's performance with and without hard limiting for different values of N , K , and F . Fig. 6(a) shows the upperbound on PE, (34), due to hard-limiting and the PE with no hard-limiting, (16), versus threshold Th for $N = 10$, $F = 1000$, and for different values of K ($K = 1, 3, 5, 7, 9$). For $K = 1$ and $Th = 1$, the performance of both systems (i.e., with and without hard-limiting) is the same, e.g., $\approx 2.24 \times 10^{-3}$. This is expected because when Th is set at 1 in the system with hard-limiting, the errors due to analog summation of light intensities can still contribute to the overall error rate. In fact, this is true for all FO-CDMA systems with different values of N , F , and K . See Fig. 6(a)–(c). But, as the value of Th is pushed up, the FO-CDMA system with hard-limiting is superior to one with no hard-limiting. For example, from Fig. 6(a) when $K = 7$ and $Th = 7$, the FO-CDMA system performance with hard-limiting is improved by 1.5 orders of magnitude.

As is apparent from all these figures, Fig. 6(a)–(c), hard-limiting is superior in performance.

Case B) Ideal Chip Asynchronous: As in Case A), an upperbound on PE for FO-CDMA with hard-limiting can be

expressed as

PE [Case B] with optical hard-limiter]

$$\begin{aligned} &\leq \frac{1}{2} \left(\frac{K}{Th} \right) \prod_{m=0}^{Th-1} \left(1 - \left[q^{N-1-m} \right. \right. \\ &\quad \left. \left. + (N-1-m)pq^{N-2-m} + \sum_{i=2}^{N-1-m} \binom{N-1-m}{i} \right. \right. \\ &\quad \left. \left. \cdot p^i q^{N-1-i-m} \left(1 - Q \left(\frac{1-i/2}{\sqrt{i/12}} \right) \right) \right] \right) \end{aligned} \quad (35)$$

where p and q are defined as in (33). Fig. 7 shows the upperbound on PE of (35) versus Th for $F = 1000$, $K = 5$, and for different values of N ($N = 10, 50$). Furthermore, in Fig. 7 we compare (35) to the performance of a FO-CDMA system in which their receivers are the simple tapped-delay lines. The system performance of FO-CDMA systems with optical hard-limiting (dashed lines) are improved by four to five orders of magnitude. For bit error rate $\approx 10^{-10}$ FO-CDMA systems without optical hard-limiting can accommodate ten users where as FO-CDMA systems with optical hard-limiting can accommodate 50 users.

VI. CONCLUSION

In this paper, we developed the probability density functions associated with $N-1$ interfering optical orthogonal codes, with which the upper and lower bounds on the probability or error per bit for FO-CDMA were achieved. Furthermore, we discussed a means of reducing the effective multiple-access interference signal by placing an optical hard-limiter at the front end of the optical correlator in a typical FO-CDMA system. We showed that FO-CDMA systems with an ideal optical hard-limiter can accommodate many more users with respect to FO-CDMA systems without the optical hard-limiter.

APPENDIX

In this Appendix we describe the mathematical development of the probability density functions associated with the interference signal $I_n^{(1)}$ s. Furthermore, we show that, mathematically, the probability density functions associated with the above interference signals are equal to the probability density functions associated with their corresponding interfering optical disk patterns [1] (see Section IV). With no loss in generality, we denote receiver one to be the desired receiver, $\tau_c = 0$, then from (6) the output of the first user's correlator Z_1 is expressed as

$$Z_1 = d_1 + \sum_{n=2}^N I_n^{(1)} \quad (A.1)$$

where the first term of (A.1), d_1 , is the desired term for the user number one and the second term, $\sum_{n=2}^N I_n^{(1)}$, is the undesired term. The desired term is expressed as $d_1 = b_0^{(1)}K$ where $b_0^{(1)}$ corresponds to the zeroth data of the first user and K corresponds to the number of pulses (weight) in the OOC's, with F chips. Each interference signal $I_n^{(1)}$ of the undesired term can be expressed as

$$\begin{aligned} I_n^{(1)} &= \frac{1}{T_c} \int_0^{\tau_n} DP_n(t - \tau_n) b_n(t - \tau_n) DP_1(t) dt \\ &\quad + \frac{1}{T_c} \int_{\tau_n}^T DP_n(t - \tau_n) b_n(t - \tau_n) DP_1(t) dt. \end{aligned} \quad (A.2)$$

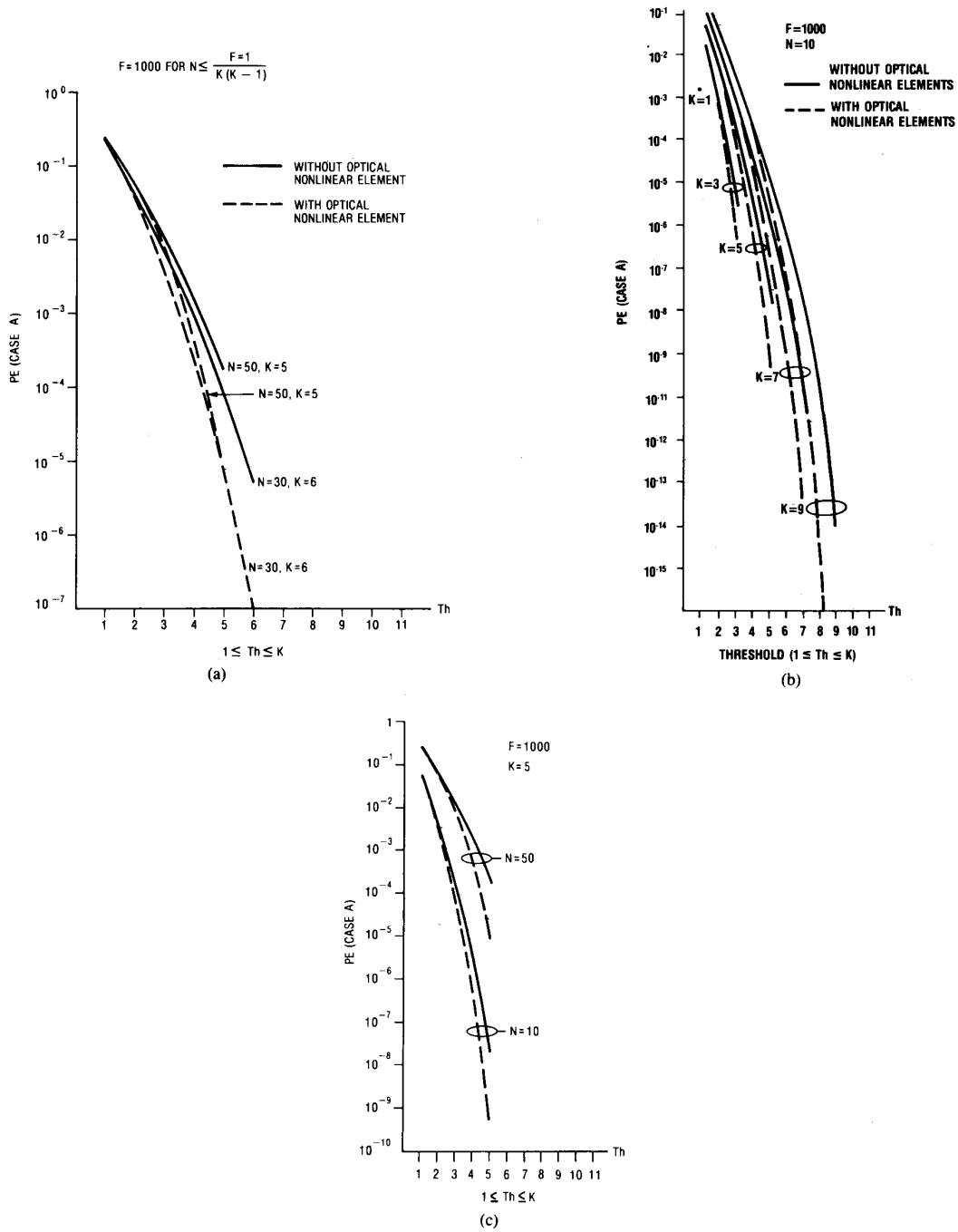


Fig. 6. (a) Upper bounds on bit error rate performance for the two cases with and without an optical hard-limiter. $F = 1000$, $N = 10$, and $K = 1, 3, 5, 7, 9$. (b) Upper bound on bit error rate performance versus threshold with and without an optical hard-limiter for $N = 50$, $K = 5$, $N = 30$, $K = 6$, and $F = 1000$. (c) Upper bound on bit error rate performance versus threshold with and without an optical hard-limiter for $F = 1000$, $K = 5$, and $N = 10, 50$.

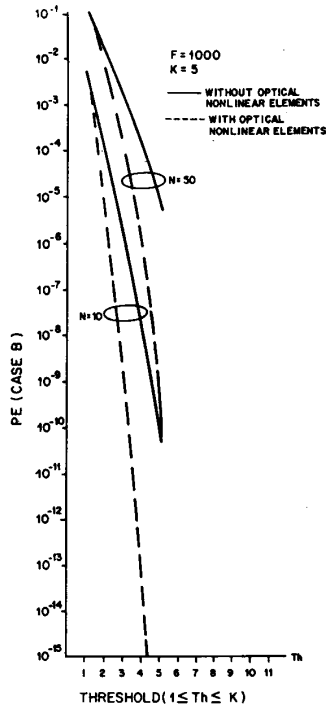


Fig. 7. Lower bound on bit error rate performance versus threshold with and without an optical hard-limiter for $F = 1000$, $K = 5$, $N = 10, 50$.

From (2) one can write the signal $b_n(t - \tau_n)$ as

$$b_n(t - \tau_n) = \begin{cases} b_{-1}^{(n)} & \text{for } 0 < t \leq \tau_n \\ b_0^{(n)} & \text{for } \tau_n < t \leq T \end{cases} \quad (\text{A.3})$$

τ_n , the time delay associated with the n th signal, is a random variable with a probability density function uniformly distributed on the interval $(0, T)$. Furthermore, τ_n can be expressed as the sum of two random variables, M_n and ρ_n , for which M_n is a random variable that can take on any integer value with equal probability between $(0, F - 1)$, and another random variable, ρ_n , that is uniformly distributed on the interval $(0, 1)$, i.e.,

$$\tau_n = (M_n + \rho_n)T_c \quad (\text{A.4})$$

ρ_n of (A.4) is defined as the epoch time associated with the n th user, and it represents the chip misalignment in time between the locally generated OOC of the desired user and the transmitted OOC of the n th user. In the following analysis of the interference signal, we consider two cases: A) chip synchronous and B) ideal chip asynchronous. In Case A), we let the epoch time ρ_n of (A.4) to be zero for all n . In Case B), ρ_n 's are independent and identically distributed random variables with a probability density function defined as before. In networks where there is no central timing control among the users, then Case A) would be an idealized case and it is considered only for its more mathematical convenience with respect to Case B). Note that chip synchronous interference signal is the worst case (see [1]).

Case A) Chip Synchronous: In this case, $I_n^{(1)}$ can be expressed as

$$I_n^{(1)} = b_{-1}^{(n)} \sum_{j=0}^{M_n-1} A_j^{(1)} A_{F-M_n+j}^{(n)} + b_0^{(n)} \sum_{j=M_n}^{F-1} A_j^{(1)} A_{j-M_n}^{(n)} \quad (\text{A.5})$$

The above random variable $I_n^{(1)}$ can take on two values, namely, one or zero [this is due to the cross correlation property of two OOC's with $\lambda_c = 1$, (see [1])]. If we let $p = P_r(I_n^{(1)} = 1)$ then, $P_r(I_n^{(1)} = 0) = 1 - P_r(I_n^{(1)} = 1) = 1 - p = q$. Therefore, the probability density function for the above random variable $I_n^{(1)}$ can be expressed as

$$P_{I_n^{(1)}}(I_n^{(1)}) = q\delta(I_n^{(1)}) + p\delta(I_n^{(1)} - 1). \quad (\text{A.6})$$

From (A.6) the expected value (or mean) of the random variable $I_n^{(1)}$ is equal to

$$E(I_n^{(1)}) = 0 \cdot P_r(I_n^{(1)} = 0) + 1 \cdot P_r(I_n^{(1)} = 1) = p \quad (\text{A.7})$$

where E denotes the mathematical expectation (ensemble average). If $b_{-1}^{(n)}$, $b_0^{(n)}$, and M_n are independent random variables then, $E(I_n^{(1)})$ of (A.5) is equal to

$$E(I_n^{(1)}) = \frac{K^2}{2F}. \quad (\text{A.8})$$

Therefore, from (A.6), (A.7), and (A.8), the probability density function for the random variable $I_n^{(1)}$ is equal to

$$P_{I_n^{(1)}}(I_n^{(1)}) = \left(1 - \frac{K^2}{2F}\right) \delta(I_n^{(1)}) + \frac{K^2}{2F} \delta(I_n^{(1)} - 1). \quad (\text{A.9})$$

Equation (A.9), is equivalent to the probability density function of [1, eq. (1)].

Case B) Ideal Chip Asynchronous: Replacing (A.4) and (A.3) into (A.2) and carrying out the integration then $I_n^{(1)}$ can be expressed as [6]

$$I_n^{(1)} = b_{-1}^{(n)} \left[\rho_n \sum_{j=0}^{M_n} A_j^{(1)} A_{F-M_n-1+j}^{(n)} + (1 - \rho_n) \sum_{j=0}^{M_n-1} A_j^{(1)} A_{F-M_n+j}^{(n)} \right] + b_0^{(n)} \left[\rho_n \sum_{j=M_n+1}^{F-1} A_j^{(1)} A_{j-M_n-1}^{(n)} + (1 - \rho_n) \sum_{j=M_n}^{F-1} A_j^{(1)} A_{j-M_n}^{(n)} \right]. \quad (\text{A.10})$$

Note that if $\rho_n = 0$, in the above equation, one would get the chip synchronous interference signal, i.e., (A.5). The expected value for the above random variable $I_n^{(1)}$ is equal to

$$E(I_n^{(1)}) = \frac{K^2}{2F}. \quad (\text{A.11})$$

In general, the probability density function for the above chip asynchronous interference signal, $I_n^{(1)}$ is given by [1, Section V]

$$P_{I_n^{(1)}}(I_n^{(1)}) = q\delta(I_n^{(1)}) + p\delta(I_n^{(1)} - 1) + (1 - p - q) \overline{I_n^{(1)}}. \quad (\text{A.12})$$

From (A.11)

$$E(I_n^{(1)}) = \frac{1 + p - q}{2}. \quad (\text{A.12})$$

If $p + q = 1$ in the above equation, then $E(I_n^{(1)}) = p$. This is equivalent to chip synchronous case (A.7). And if $p = 0$ in (A.12), then $E(I_n^{(1)}) = (1 - q)/2$. This corresponds to the interference of two OOC's for which there are no adjacent

pulses, i.e., ideal chip asynchronous interference. And for this case $q = 1 - K^2/F$. Therefore, the probability density function for interference signal $I_n^{(i)}$ in this case, can be written as

$$P_{I_n^{(i)}}(I_n^{(i)}) = \left(1 - \frac{K^2}{F}\right) \delta(I_n^{(i)}) + \frac{K^2}{F} |I_n^{(i)}|. \quad (\text{A.13})$$

Equation (A.13) is equivalent to the probability density function defined as in [1, eq. (21)].

REFERENCES

- [1] J. A. Salehi, "Code division multiple-access techniques in optical fiber networks—Part I: Fundamental principles," *IEEE Trans. Commun.*, see this issue, pp. 824–833.
- [2] F. R. K. Chung, J. A. Salehi, and V. K. Wei, "Optical orthogonal codes: Design, analysis and applications," *IEEE Int. Symp. on Inform. Theory*, Ann-Arbor, MI, 1986; also *IEEE Trans. Inform. Theory*, May 1989.
- [3] M. B. Pursley, *Spread-Spectrum Multiple-Access Communications in Multi-User Communication Systems*, G. Longo, Ed. New York: Springer-Verlag, 1981, pp. 130–199.
- [4] E. Marom, "Optical delay line matched filters," *IEEE Trans. Circuits Syst.*, vol. CAS-25, pp. 360–364, June 1978.
- [5] A. A. Sawchuk, T. C. Strand, "Digital optical computing," *Proc. IEEE*, Special Issue on Optical Computing, pp. 758–779, July 1984.
- [6] J. A. Salehi, "Spread spectrum multiple access systems performance analysis," U.S.C., Ph.D. dissertation, 1984.

Jawad A. Salehi (M'80–M'84), for a photograph and biography, see this issue, p. 833.

★



Charles A. Brackett (S'60–M'64) received the Ph.D. degree in electrical engineering from the University of Michigan, Ann Arbor, in 1968.

From 1968 to 1984, he was employed at AT&T Bell Laboratories. There he initially worked on semiconductor microwave oscillators. Beginning in 1974, he was involved in optical component development, including optical receivers for transmission systems and optical data links for electronic switching systems. In 1980, he assumed responsibility for the final development of all optical receivers designed by AT&T Bell Laboratories. He joined Bell Communications Research, Morristown, NJ, in October 1983, as District Manager of Optical Networks Research where he began work on the use of multiwavelength technology in the exchange network and optical code-division multiple access networks. He is now responsible for architectures to provide increased network flexibility and capability. His interests include optical transmission technology, optical networks, and optical switching.

Dr. Brackett is a member of Tau Beta Pi, Eta Kappa Nu, Sigma Xi, and Phi Kappa Phi.